arXiv:1409.6887v2 [cond-mat.mtrl-sci] 26 Sep 2014

Origin of traps and charge transport mechanism in hafnia

D. R. Islamov,[1,2,*] V. A. Gritsenko,[1,2,†] C. H. Cheng,[3] and A. Chin[4,‡]

[1] *Rzhanov Institute of Semiconductor Physics, Siberian Branch of Russian Academy of Sciences, Novosibirsk, 630090, Russian Federation*
[2] *Novosibirsk State University, Novosibirsk, 630090, Russian Federation*
[3] *Dept. of Mechatronic Technology, National Taiwan Normal University, Taipei, 106, Taiwan ROC*
[4] *National Chiao Tung University, Hsinchu, 300, Taiwan ROC*

(Dated: September 29, 2014)

In this study, we demonstrated experimentally and theoretically that oxygen vacancies are responsible for the charge transport in HfO_2. Basing on the model of phonon-assisted tunneling between traps, and assuming that the electron traps are oxygen vacancies, good quantitative agreement between the experimental and theoretical data of current-voltage characteristics were achieved. The thermal trap energy of 1.25 eV in HfO_2 was determined based on the charge transport experiments.

PACS numbers: 77.55.df, 77.84.Bw, 72.20.−i, 72.20.Jv
Keywords: hafnium oxide, transport, traps, oxygen vacancy

Knowledge about charge transport mechanisms hafnia (hafnium oxide, HfO_2) is crucial for modern microelectronics, because high-κ HfO_2 is used as a gate dielectric in high-speed MOSFETs [1, 2] and FinFETs [3, 4] and a blocking insulator in Si-oxide-nitride-oxide-silicon-type (SONOS) flash memory cells [5, 6]. Hafnia is a promising candidate to used sa active medium in resistive random access memory, which would involve combining the most favorable properties of both high-speed dynamic random access memory and non-volatile flash memory [7–9]. However, an unresolved physics is the nature of defects and traps that are responsible for the charge transport in HfO_2. The atomic structure of defect that affects the localization and charge transport still remains unclear. Currently, the accepted hypothesis is that oxygen vacancies are responsible for charge transport in dielectric. Although many studies have investigated the theory of the atomic and electronic structure of oxygen vacancies in hafnia [10–17], direct experimental data regarding the presence of oxygen vacancies in hafnia were reported recently [18]. It was shown that oxygen vacancies in hafnia are responsible for blue luminescence band at 2.7 eV and a luminescence excitation band at 5.2 eV, and a hypothesis that the oxygen vacancies in hafnia act as traps in charge transport through the dielectric was discussed [18]. In this case thermal energy traps in HfO_2 is equal to a half of the Stokes luminescence shift $W_t = (5.2 - 2.7)/2 = 1.25$ eV.

A lot of charge transport studies described experiment results by Pool-Frenkel (PF) mechanism in hafnia-based structures [19–21]. However, the most investigations explained their results qualitatively, and did not get quantitative agreement of the phenomenological parameters such as dynamic permittivity, trap energy, frequency factor etc. The most part of transport investigations did not get into account neither charge trap density, which depends on thin film fabrication technology, nor phonon influence on electron and hole transport, which might be significant at high temperatures.

In this letter, we phonon-assisted tunneling between traps conduction mechanism in HfO_2 was developed with good quantitative as well as qualitative agreement. It was clearly shown that oxygen vacancies are responsible for the charge transport in HfO_2 and HfO_2-based devices.

Transport measurements were performed for metal-insulator-semiconductor (MIS) and metal-insulator-metal (MIM) structures. For the MIS Si/HfO_x/Ni structures, the 20-nm-thick amorphous hafnia was deposited on a n-type Si (1 0 0) wafer by using the atomic layer deposition (ALD) system. Tetrakis dimethyl amino hafnium (TDMAHf) and water vapor were used as precursors at a chamber temperature of 250°C for HfO_x film deposition.

Another set of MIS samples with 8-nm-thick HfO_x films was fabricated using physical vapor deposition (PVD). A pure HfO_2 target was spattered by an electron beam, and HfO_2 were deposited on the n-type Si (1 0 0) wafer. Low temperature post-deposition annealing (PDA) during 15 min at 400°C was applied to prevent the growth of interfacial SiO_x [22]. Structural analysis shows that the resulting HfO_x films were amorphous. To fabricate Si/TaN/HfO_x/Ni MIM structures, we deposited the 8-nm-thick amorphous hafnia on 100-nm-thick TaN films on Si wafers, using PVD. We did not apply any post-deposition annealing to produce the most non-stoichiometric films. All samples for transport measurements were equipped with round 50-nm-thick Ni gates with a radius of 70 μm. Transport measurements were performed using a Hewlett Packard 4155B semiconductor parameter analyzer and an Agilent E4980A precision LCR meter.

The experimental current-voltage (I-V) characteristics in MIS(PVD) structures, measured at different temperatures T with a positive bias applied to the Ni contact, are shown in Fig. 1, graphed by different characters in PF ($\log(I)$-$\sqrt{V}$) plot. The current grows exponentially with increasing of the gate voltage and temperature. We

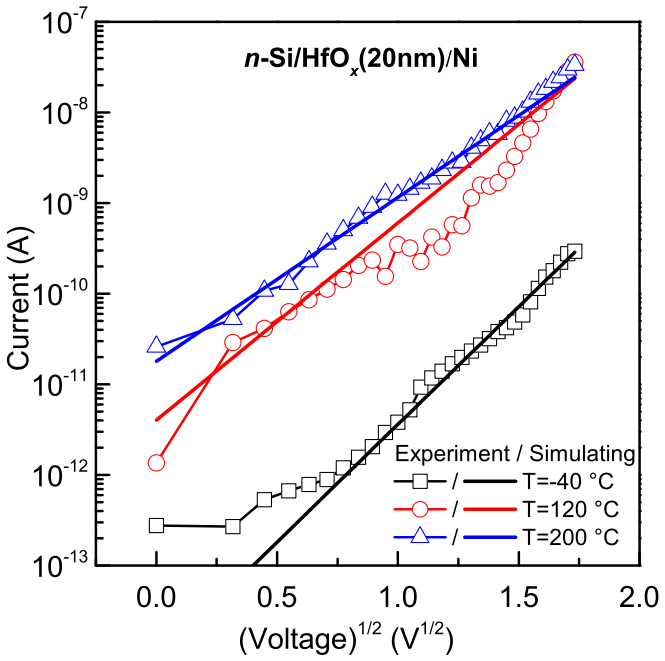

FIG. 1. (Color online) Experimental current-voltage characteristics (characters) of n-Si/HfO_x/Ni MIS(PVD) structure and simulation (lines) by Frenkel model of the trap ionization (1), (2) at different temperatures on PF plot.

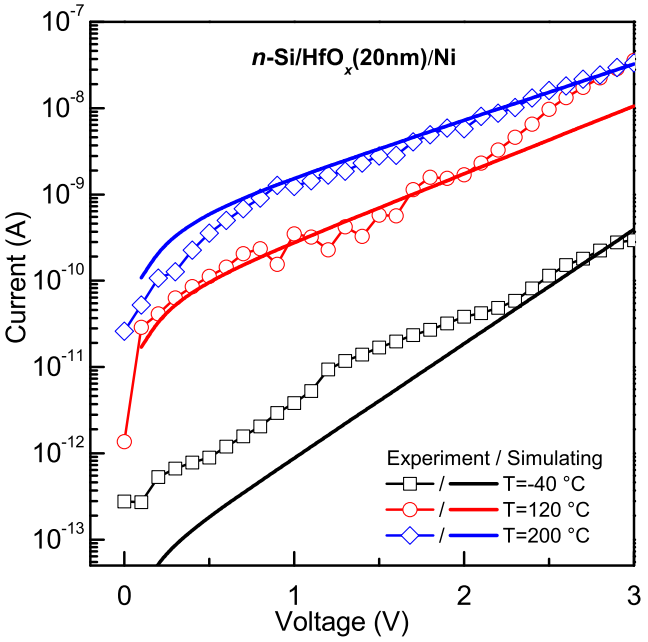

FIG. 2. (Color online) Experimental current-voltage characteristics (characters) of n-Si/HfO_x/Ni MIS(PVD) structure and simulation (lines) by phonon-assisted tunneling between traps (3) at different temperatures.

attempted to explain the experimental data by using isolated trap ionization model:

$$J = eN^{2/3}P, \tag{1}$$

where J is the current density, e is the electron charge, N is the charge trap density, P is the probability of trap ionization per second, and has different dependencies on electric field F and temperature. In term of PF model the probability is

$$P = \nu \exp\left(-\frac{W_\mathrm{t} - \beta_\mathrm{PF}\sqrt{F}}{kT}\right). \tag{2}$$

ν is the frequency factor which was defined as $\nu \simeq W_\mathrm{t}/h$, W_t is thermal trap energy (the energy of thermal ionization of the trap), h is the Planck constant, β_PF is PooleFrenkel coefficient, is the electric field, and k is the Boltzmann constant [23]. Experimental I-V characteristics and results of the fitting procedure are shown in Fig. 1. As can be seen, Frenkel model (2) describes the experiment data qualitatively very good. However, quantitative fitting procedure returns nonphysical fitting parameter values: the slopes of the fitting lines with Poole-Frenkel coefficient $\beta_\mathrm{PF} = e^3/\pi\varepsilon_0\varepsilon_\infty$ give the dynamic permittivity $\varepsilon_\infty(T) = 10 \div 20$, which is much higher than $\varepsilon_\infty(\mathrm{HfO_2}) = 4$. ε_0 is vacuum permittivity (dielectric constant). Further fittings return $N \sim 4\,\mathrm{cm}^{-3}$ (!) and $W_\mathrm{t} = 0.3 \div 0.4\,\mathrm{eV}$. Found values the charge trap density of $N \sim 4\,\mathrm{cm}^{-3}$ at $\nu \simeq W_\mathrm{t}/h \sim 10^{14}\,\mathrm{s}^{-1}$ corresponds to one trap per $\sim$ 2600 Ni contacts, thus this is unrealistic value. This Taking these into account it was concluded that despite the fact that PF model describes the experiment data qualitatively, there is no quantitative agreement between experiments and theory. We tried to describe our experiments with other charge transport models in dielectrics; Hill model of overlapped traps ionization [24], and the model of multiphonon trap ionization [25]. However, the fitting procedures involved in these models returned the nonphysical fitting parameter values as well as PF model.

To describe the experiments quantitatively and qualitatively, we performed simulations based on the model of phonon-assisted tunneling between traps [26]. In this model the probability of electron tunneling between traps per second is defined as following:

$$P = \frac{\sqrt{2\pi}\hbar W_\mathrm{t}}{m^* s^2\sqrt{W_\mathrm{opt} - W_\mathrm{t}}} \exp\left(-\frac{W_\mathrm{opt} - W_\mathrm{t}}{2kT}\right) \times \\ \times \exp\left(-\frac{2s\sqrt{m^* W_\mathrm{t}}}{\hbar}\right) \sinh\left(\frac{eFs}{2kT}\right), \tag{3}$$

$\hbar = h/2\pi$, W_opt is the energy of optical excitation of the trap, m^* is the effective mass, $s = N^{-1/3}$ is mean distance between traps. The results of this multi-parameter fitting procedure are shown in Fig.2, graphed in solid lines. This procedure yielded the values of different transport parameters, $N = 6.8 \times 10^{19}\,\mathrm{cm}^{-3}$, $W_\mathrm{t} = 1.25\,\mathrm{eV}$, $W_\mathrm{opt} = 2W_\mathrm{t} = 2.5\,\mathrm{eV}$, and $m^* = (0.3 \div 0.4)m_\mathrm{e}$ (m_e is

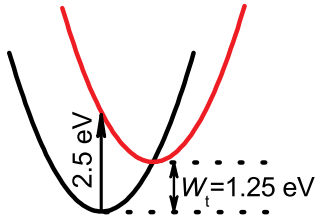

FIG. 3. (Color online) Configuration coordination energy diagram of trap ionization process on negative charged oxygen vacancy in hafnia (lower term is filled ground state, upper term is excited empty state).

a free electron mass). Quantitatively, there is full agreement between the model of phonon-assisted tunneling between traps and the experimental data. The trap thermal energy value of 1.25 eV that was obtained is close to that of 1.2 eV [27] and $W_t = 1.36$ eV [28] observed earlier, and equal to a half of the Stokes luminescence shift [18]. Furthermore, the trap optical energy value of $W_{opt} = 2.5$ eV is close to the calculated value of 2.35 eV for the negatively charged oxygen vacancy in hafnia reported earlier [14].

Fig. 3 shows the configuration diagram of a negatively charged oxygen vacancy (electron trap) in hafnia. A vertical transition with a value of 2.5 eV corresponds to the optical trap excitation, transitions of 1.25 eV correspond to thermal trap energy.

The same procedure was applied to experiment data of the charge transport measurements in MIS(ALD) and MIM structures. Experiment current-voltage characteristics compared with simulations in terms of the model of phonon-assisted tunneling between traps in MIS(ALD) are shown in Fig. 4. Fitting procedure returns the following parameters values: $N = 2.5 \times 10^{20}$ cm^{-3}, $W_t = 1.25$ eV, $W_{opt} = 2W_t = 2.5$ eV, and $m^* = 0.8m_e$. Different values of fitting parameters of MIS(ALD) and MIS(ALD) structures have only the trap density N and effective mass m^*. The difference of effective mass values is due to bulk space charge (due to captured in traps electrons and holes), which is adequately addressed in [29]. Neither thermal trap energy nor optical trap energy depend on film fabrication technology.

Fig. 5 shows the experimental data of current-voltage measurements in MIM structures at different temperatures. The solid lines present the results of simulations in terms of phonon-assisted tunneling between traps (3). MIM structures have the following parameter values: $N = 5.5 \times 10^{20}$ cm^{-3}, $W_t = 1.25$ eV, $W_{opt} = 2W_t = 2.5$ eV, and $m^* = 0.9m_e$.

An artifact feature of experimental I-V-T curves that the zero current is observed at non zero but negative voltages as shown in Fig. 5. This phenomenon is due to

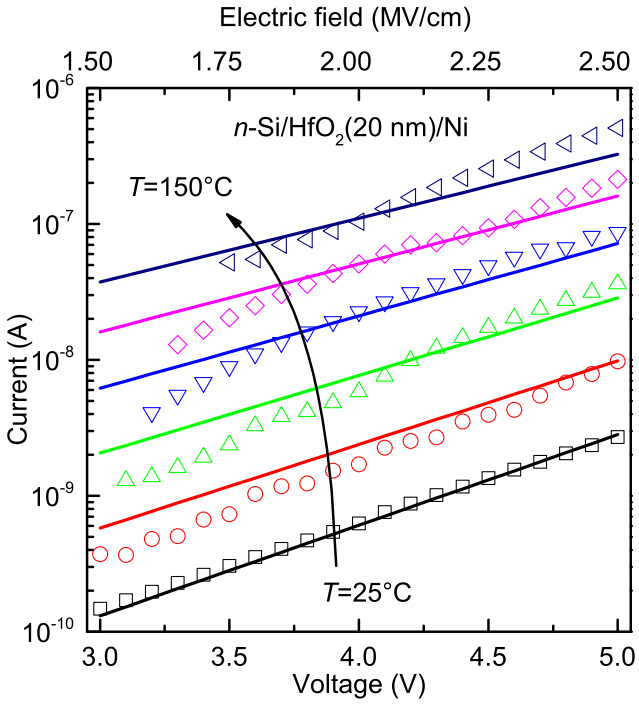

FIG. 4. (Color online) Experimental current-voltage characteristics (characters) of n-Si/HfO$_x$/Ni MIS(ALD) structure and simulation (lines) by phonon-assisted tunneling between traps (3) at different temperatures.

displacement current

$$I_D = C \cdot dV/dt, \tag{4}$$

C is capacity of the sample, $dV/dt = +0.3$ V/s is voltage sweep rate. Taking into account (4) in simulation of I-V-T characteristics (1), (3) with found fitting parameters the artifact feature is described with good agreement as shown by dashed lines in Fig. 5.

The difference between different MIS ad MIM structures in effective mass is due to bulk space charge. However, it is important to notice that the trap's energy parameters are invariants of grown structures and film fabrication techniques. Consequently, we found that the nature of charge carrier transport in hafnia and hafnia-based structures is phonon-assisted tunneling between traps. This charge transport model is more simple than based in quasi-continuous spectra of charge trap energy 1.4 – 2.4 eV, proposed by L. Vandelli *et al.* [30].

These results combined with spectra measurements and quantum chemical simulations [18] show that namely oxygen vacancies are responsible for charge transport in HfO$_x$, and the oxygen vacancies play the role or charge traps.

Previous experiments in charge transfer have demonstrated that hafnia conductivity is bipolar (or two-band)

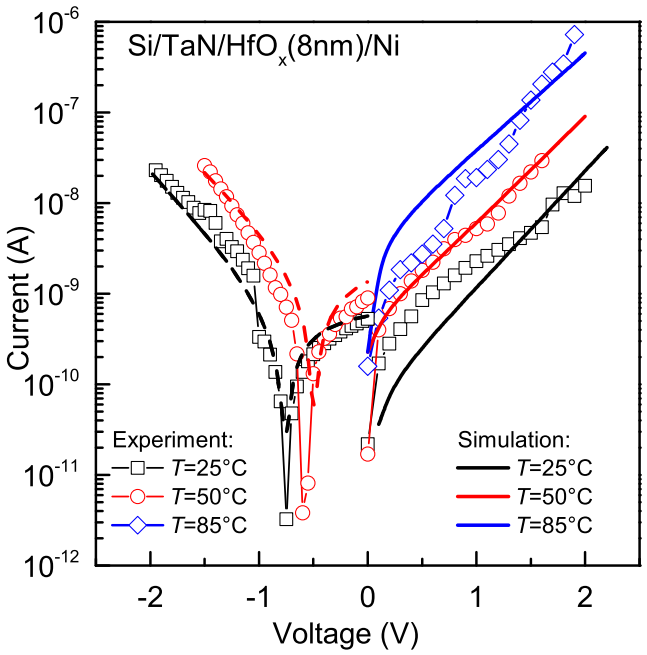

FIG. 5. (Color online) Experimental current-voltage characteristics (characters) in Si/TaN/HfO_x/Ni MIM structures at different temperatures. Black, red and blue solid lines represent I-V simulations by phonon-assisted tunneling between traps at positive bias. Dashed lines show I-V simulations taking into account displacement current (4).

[30–32]: electrons are injected from a negatively shifted contact in the dielectric, and holes are injected from a positively shifted electrode in the dielectric. For the reason of simplicity, the current study took into account electron conductivity only.

To summarize, we examined the transport mechanisms of HfO_2, demonstrating that transport in hafnium oxide is described by the model of phonon-assisted tunneling between traps. Simulating the current-voltage characteristics of this model and comparing experimental data with calculations revealed the energy parameters of the traps in hafnia: the thermal trap energy of 1.25 eV and the optical trap energy of 2.5 eV. Phonon-assisted tunneling between traps charge transport model describe experiment data results with excellent qualitative and quantitative agreement, while standard PF model has qualitative agreement only with unrealistic values for material parameters. These results jointly with earlier ones [18] facilitated determining that oxygen vacancies act as charge carrier traps.

Our results can be used to predict the leakage currents in HfO_2-based devices and applications. High-quality MOSFET and FinFET transistors and SONOS flash memory require low leakage currents through the gate dielectrics and blocking insulator, while different states in resistive memory cells must be distinguishable over a wide range of temperatures. Temperature dependence of memory window (resistance ratio in different states) in resistive memory might be predicted as well.

This work was particularly supported by National Science Council, Taiwan (grant No. NSC103-2923-E-009-002-MY3) (growing test structures, preparing samples, performing transport measurements), and by the Russian Science Foundation (grant No. 14-19-00192) (calculations, modeling).

* damir@isp.nsc.ru
† grits@isp.nsc.ru
‡ albert_achin@hotmail.com

[1] T. P. Ma, H. M. Bu, X. W. Wang, L. Y. Song, W. He, M. Wang, H.-H. Tseng, and P. J. Tobin, IEEE Trans. Device Mater. Rel. **5**, 36 (2005).
[2] J. Robertson, Reports on Progress in Physics **69**, 327 (2006).
[3] M. A. Pavanello, J. A. Martino, E. Simoen, R. Rooyackers, N. Collaert, and C. Claeys, Solid-State Electronics **51**, 285 (2007).
[4] A. Tsormpatzoglou, D. H. Tassis, C. A. Dimitriadis, M. Mouis, G. Ghibaudo, and N. Collaet, Semiconductor Science and Technology **24**, 125001 (2009).
[5] L.-J. Chen, Y.-C. Wu, J.-H. Chiang, M.-F. Hung, C.-W. Chang, and P.-W. Su, IEEE Trans. Nanotechnol. **10**, 260 (2011).
[6] P.-H. Tsai, K.-S. Chang-Liao, T.-C. Liu, T.-K. Wang, P.-J. Tzeng, C.-H. Lin, L. S. Lee, and M.-J. Tsai, IEEE Electron Device Lett. **30**, 775 (2009).
[7] J. J. Yang, M. D. Pickett, X. Li, D. A. A. Ohlberg, D. R. Stewart, and R. S. Williams, Nature Nanotechnology **3**, 429 (2008).
[8] L. Goux, P. Czarnecki, Y. Y. Chen, L. Pantisano, X. P. Wang, R. Degraeve, B. Govoreanu, D. J. Jurczak, M.and Wouters, and L. Altimime, Applied Physics Letters **97**, 243509 (2010).
[9] Z. Wang, H. Y. Yu, X. A. Tran, Z. Fang, J. Wang, and H. Su, Physical Review B **85**, 195322 (2012).
[10] S. Guha and V. Narayanan, Physical Review Letters **98**, 196101 (2007).
[11] D. Muñoz Ramo, A. L. Shluger, J. L. Gavartin, and G. Bersuker, Physical Review Letters **99**, 155504 (2007).
[12] A. S. Foster, F. Lopez Gejo, A. L. Shluger, and R. M. Nieminen, Physical Review B **65**, 174117 (2002).
[13] J. X. Zheng, G. Ceder, T. Maxisch, W. K. Chim, and W. K. Choi, Physical Review B **75**, 104112 (2007).
[14] D. Muñoz Ramo, J. L. Gavartin, A. L. Shluger, and G. Bersuker, Physical Review B **75**, 205336 (2007).
[15] H. Jiang, R. I. Gomez-Abal, P. Rinke, and M. Scheffler, Physical Review B **81**, 085119 (2010).
[16] K. Xiong, J. Robertson, M. C. Gibson, and S. J. Clark, Applied Physics Letters **87**, 183505 (2005).
[17] P. Broqvist and A. Pasquarello, Applied Physics Letters **89**, 262904 (2006).
[18] T. V. Perevalov, V. S. Aliev, V. A. Gritsenko, A. A. Saraev, V. V. Kaichev, E. V. Ivanova, and M. V. Zamoryanskaya, Applied Physics Letters **104**, 071904 (2014).
[19] S. K. Sahoo and D. Misra, Journal of Applied Physics

110, 084104 (2011).
[20] S. Pan, S.-J. Ding, Y. Huang, Y.-J. Huang, D. W. Zhang, L.-K. Wang, and R. Liu, Journal of Applied Physics **102**, 073706 (2007).
[21] W. J. Zhu, T.-P. Ma, T. Tamagawa, J. Kim, and Y. Di, IEEE Electron Device Lett. **23**, 97 (2002).
[22] S. H. Lin, C. H. Cheng, F. S. Chen, W. B.and Yeh, and A. Chin, IEEE Electron Device Lett. **30**, 999 (2009).
[23] J. Frenkel, Physical Review **54**, 647 (1938).
[24] R. M. Hill, Philosophical Magazine **23**, 59 (1970).
[25] S. Makram-Ebeid and M. Lannoo, Physical Review B **25**, 6406 (1982).
[26] K. A. Nasyrov and V. A. Gritsenko, Journal of Applied Physics **109**, 093705 (2011).
[27] H. Takeuchi, D. Ha, and T.-J. King, Journal of Vacuum Science and Technology A **22**, 1337 (2004).
[28] D. S. Jeong and C. S. Hwang, Physical Review B **71**, 165327 (2005).
[29] K. A. Nasyrov, S. S. Shaimeev, V. A. Gritsenko, and J. H. Han, Journal of Applied Physics **105**, 123709 (2009).
[30] L. Vandelli, A. Padovani, L. Larcher, R. G. Southwick, W. B. Knowlton, and G. Bersuker, IEEE Trans. Electron Devices **58**, 2878 (2011).
[31] D. R. Islamov, V. A. Gritsenko, C. H. Cheng, and A. Chin, Applied Physics Letters **99**, 072109 (2011).
[32] T. Ando, N. D. Sathaye, K. V. R. M. Murali, and E. A. Cartier, IEEE Electron Device Lett. **32**, 865 (2011).